

# Laser probing of Cooper-paired trapped atoms

G.M. Bruun<sup>1</sup>, P. Törmä<sup>2</sup>, M. Rodriguez<sup>2</sup> and P. Zoller<sup>3</sup>

<sup>1</sup>*Nordita, Blegdamsvej 17, 2100 Copenhagen, Denmark*

<sup>2</sup>*Laboratory of Computational Engineering, P.O.Box 9400, FIN-02015 Helsinki University of Technology, Finland*

<sup>3</sup>*Institute for Theoretical Physics, University of Innsbruck, Technikerstraße 25, A-6020 Innsbruck, Austria*

We consider a gas of trapped Cooper-paired fermionic atoms which are manipulated by laser light. The laser induces a transition from an internal state with large negative scattering length (superfluid) to one with weaker interactions (normal gas). We show that the process can be used to detect the presence of the superconducting order parameter. Also, we propose a direct way of measuring the size of the gap in the trap. The efficiency and feasibility of this probing method is investigated in detail in different physical situations.

05.30.Fk, 32.80.-t, 74.25.Gz

## I. INTRODUCTION

Recent experiments on cooling and trapping Fermionic atoms have opened up new opportunities for studying fundamental quantum statistical and many-body physics. Trapped Fermionic <sup>40</sup>K atoms were cooled down to temperatures where the Fermi degeneracy sets in [1]. Two lithium isotopes were trapped simultaneously in an magneto-optical trap in [2] and optical trapping of fermionic lithium has been achieved as well [3]. The richness of the internal energy structure of the atoms and the possibility to accurately and efficiently manipulate these energy states by laser light and magnetic fields allows excellent control of these gases. Furthermore, atomic gases are dilute and weakly interacting thus offering the ideal tool for developing and experimentally testing theories of many-body quantum physics.

The degenerate Fermi gas is expected to show many interesting phenomena in its thermodynamics [4], excitation spectrum [5–8], collisional dynamics [9] and scattering of light [1,10,11]. A major goal is to observe the predicted [12,13] BCS-transition for Fermionic atoms – this would compare to the experimental realization of atomic Bose-Einstein condensates [14]. It is still, however, an open question how to observe the BCS-transition, because the value of the superconducting order parameter (gap) is expected to be small and the existence of the order parameter does not significantly change the density profile and other bulk properties of the gas.

There are several proposals for measuring the superconducting order parameter. Off-resonant light scattering as a probe was proposed in [15,16]. Superfluidity is predicted to effect both the spectral and spatial distribution of the scattered light. In [17], superfluidity was found to increase the optical lineshift and linewidth. Also non-optical phenomena, such as collective and single particle excitations, have been proposed to be used for observing the BCS-transition [18–22]. Probing by a magnetic field was considered in [23].

The use of on-resonant light as a probe for the order pa-

rameter was proposed in [24]. The basic idea is to transfer atoms from one internal (hyperfine) state for which the atoms are Cooper paired to another state for which the interatomic interaction is not strong enough to lead to a BCS state. This effectively creates a superconducting – normal state interface across which the atomic population can move. There is a conceptual analogy to electron tunneling from a superconducting metal to a normal one which is used to measure the gap and the density of states for Cooper-paired electrons [25]. The tuneability of the interaction strengths which is required for this scheme is obtained by the use of magnetic fields. This allows to manipulate the scattering lengths between atoms in different internal states, see e.g. the recent experimental results concerning optically trapped fermionic Lithium atoms [3] and the theory predictions for <sup>40</sup>K [26].

The basic idea in the proposal [24] is that the absorption peak is shifted and becomes asymmetric because of the existence of the gap – the laser has to provide energy for breaking the Cooper pairs in order to transfer atoms from the paired state to the unpaired one. This behaviour is, however, strongly influenced by the specific physical situation. In this paper we investigate in detail how the choice of the chemical potentials for the superfluid and the normal state, and the choice of the interaction strengths and laser profiles affect the absorption. We also compare the results in the cases of a homogeneous system and a trapped gas. In section II, we introduce the considered system. The linear response of the gas for a light probe is derived in section III, both for a homogeneous and a trapped gas. In section IV the various parameters that affect the observed absorption are discussed. In section V exact numerical results are presented for the limit when the laser beam profile can be considered a constant. A beam profile with non-zero intensity only in a small volume in the middle of the trap is considered in section VI. This case is very interesting because then only the center of the trap is probed. Thus the order parameter seen by the laser is almost constant and indeed, we find a remarkable agreement with the re-

sults predicted for a homogeneous system. We finally summarize the results in section VII.

## II. THE SUPERCONDUCTOR - NORMAL STATE INTERFACE

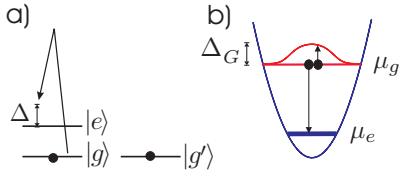


FIG. 1. Probing of the gap in a gas of attractively interacting cold Fermionic atoms. a) Laser excitation with the coupling  $\Omega$  and the detuning  $\Delta$  transfers a Cooper paired atom from the internal state  $|g\rangle$  to the state  $|e\rangle$ . b) The other atom in the initial Cooper pair becomes an excitation in the BCS state, therefore the laser has to provide also the additional gap energy  $\Delta_G$ . In this picture the Fermi levels  $\mu_g$  and  $\mu_e$  for the internal states have been chosen to be different from each other but they could also be equal.

We consider atoms with three internal states available, say  $|e\rangle$ ,  $|g\rangle$ , and  $|g'\rangle$ . They are chosen so that the interaction between atoms in states  $|g\rangle$  and  $|g'\rangle$  is relatively strong and their chemical potentials are nearly equal so that  $|g\rangle$  and  $|g'\rangle$  can be assumed to be Cooper-paired. All other interactions are small enough and/or the chemical potentials of the corresponding states are different enough in order to assume the  $|e\rangle$  atoms to be in a normal state [12]. The laser frequency is chosen to transfer population between  $|e\rangle$  and  $|g\rangle$ , but is not in resonance with any transition which could move population away from the state  $|g'\rangle$ .

For small intensities, the laser-interaction can be treated as a perturbation, the unperturbed states being the normal and the superconducting state. The transfer of atoms from  $|g\rangle$  to  $|e\rangle$  is then analogous to tunneling of electrons from a normal metal to a superconductor induced by an external voltage, which can be used as a method to probe the gap and the density of states of the superconductor [25]. In our case the tunneling is between two internal states rather than two spatial regions, this resembles the idea of internal Josephson-oscillations in two-component Bose-Einstein condensates [27]. Fig. 1 illustrates the basic idea. The observable carrying essential information about the superconducting state is the change in the population of the state  $|e\rangle$ , we call this the current  $I$ .

We define a two-component Fermion field

$$\psi(\mathbf{x}) = \begin{pmatrix} \psi_e(\mathbf{x}) \\ \psi_g(\mathbf{x}) \end{pmatrix}, \quad (1)$$

where  $\psi_e$  and  $\psi_g$  fulfill standard Fermionic commutation relations. The fields  $\psi_{e/g}$  can be expanded using some

basis functions (e.g. plane waves or trap wave functions) and corresponding creation and annihilation operators:  $\psi_{e/g}(\mathbf{x}) = \sum_j c_j^{e/g} \phi_j^{e/g}(\mathbf{x})$ . The annihilation and creation operators fulfil  $\{c_i^e, c_j^g\} = 0$  and  $\{c_i^{e/g\dagger}, c_j^{e/g}\} = \delta_{ij}$ . The two components of the field, corresponding to the internal states  $|e\rangle$  and  $|g\rangle$ , are coupled by a laser. This can be either a direct excitation or a Raman process; we denote the atomic energy level difference by  $\omega_a$  ( $\hbar \equiv 1$ ), the laser frequency  $\omega_L$  and the wave vector  $k_L$  – in the case of a Raman process these are effective quantities. In the rotating wave approximation the Hamiltonian reads

$$H = H_e + H_{gg'} + \frac{\Delta}{2} \int d^3x \psi^\dagger(\mathbf{x}) \sigma_z \psi(\mathbf{x}) + \int d^3x \psi^\dagger(\mathbf{x}) \begin{pmatrix} 0 & \Omega(\mathbf{x}) \\ \Omega^*(\mathbf{x}) & 0 \end{pmatrix} \psi(\mathbf{x}). \quad (2)$$

Here  $\Delta = \omega_a - \omega_L$  is the (effective) detuning, and  $\Omega(\mathbf{x})$  contains the spatial dependence of the laser field multiplied with the (effective) Rabi frequency. The parts  $H_e$  and  $H_{gg'}$  contain terms which depend only on  $\psi_e$  or  $\psi_g$ ,  $\psi_{g'}$ , respectively. Possible spatial inhomogeneity, e.g. from the trap potential, is also included in  $H_e$  and  $H_{gg'}$ .

## III. THE CURRENT

The observable carrying essential information about the superconducting state is the rate of change in population of the  $|e\rangle$  state. We may call it, after the electron tunneling analogy, the current

$$I(t) = -\langle \dot{N}_e \rangle,$$

where  $N_e = \int d^3x \psi_e^\dagger(\mathbf{x}) \psi_e(\mathbf{x})$ . The current  $I(t)$  is calculated considering the tunneling part of the Hamiltonian,

$$H_T = H - (H_e + H_{gg'} + \Delta/2(N_e - N_g))$$

as a perturbation; the current  $I$  becomes the first order response to the external perturbation caused by the laser. We calculate it both in the homogeneous case and in the case of harmonic confinement. The calculations are done in the grand canonical ensemble, therefore the chemical potentials  $\mu_g$  and  $\mu_e$  are introduced. Also the detuning  $\Delta$  acts like a difference in chemical potentials, thus it becomes useful to define an effective quantity of the form  $\tilde{\Delta} = \mu_e - \mu_g + \Delta \equiv \Delta\mu + \Delta$ . In the derivation we assume finite temperature, but most of the results will only be quoted for  $T=0$ .

### A. Homogeneous case

The assumption of spatial homogeneity is appropriate when the atoms are confined in a trap potential which

changes very little compared to characteristic quantities of the system, such as the coherence length and the size of the Cooper pairs. In the present context, this assumption is also valid when the laser profile is chosen so that it only probes the middle of the trap where the order parameter is nearly constant in space – this will be discussed in more detail in section VI.

In the homogeneous case the Fermion fields  $\psi_{e/g}$  can be expanded into plane waves. The Hamiltonian becomes

$$H = H_e + H_{gg'} + \frac{\Delta}{2} \sum_k [c_k^{e\dagger} c_k^e - c_k^{g\dagger} c_k^g] + \sum_{kl} [T_{kl} c_k^{e\dagger} c_l^g + h.c.], \quad (3)$$

where

$$T_{kl} = \frac{1}{V} \int d^3x \Omega(\mathbf{x}) e^{i\mathbf{k}\cdot\mathbf{x}} e^{-i\mathbf{l}\cdot\mathbf{x}}.$$

We calculate the current

$$I = -\langle \dot{N}_e \rangle = -i\langle [H, N_e] \rangle \quad (4)$$

treating  $H_T$  as a perturbation: terms of higher order than  $H_T^2$  are neglected. Because we are interested in the current between the superconducting and normal states, correlations of the form  $\langle c_e^\dagger c_e c_g c_g \rangle$  (and *h.c.*) are omitted since they correspond to tunneling of pairs (Josephson current). The current can be written

$$I = \int_{-\infty}^{\infty} dt \theta(t) (e^{-i\tilde{\Delta}t} \langle [A^\dagger(0), A(t)] \rangle - e^{i\tilde{\Delta}t} \langle [A(0), A^\dagger(t)] \rangle)$$

where  $A(t) = \sum_{kl} T_{kl} c_k^{g\dagger}(t) c_l^e(t)$ , and  $c_l^{e/g}(t) = e^{iKt} c_l^{e/g} e^{-iKt}$  where  $K = H - H_T - \mu_e N_e - \mu_g N_g$ . The two terms in the above equation have the form of retarded and advanced Green's functions. These are evaluated using Matsubara Green's functions techniques, which leads to

$$I = \sum_{kl} |T_{kl}|^2 \int_{-\infty}^{\infty} \frac{d\epsilon}{2\pi} [n_F(\epsilon) - n_F(\epsilon + \tilde{\Delta})] A_g(k, \epsilon + \tilde{\Delta}) A_e(l, \epsilon),$$

where  $n_F$  are the Fermi distribution functions and  $A_{g/e}$  are the spectral functions for the superconducting and normal states. We use the standard expressions [25]

$$A_e(l, \epsilon) = 2\pi\delta(\epsilon - \xi_l)$$

and

$$A_g(k, \epsilon + \tilde{\Delta}) = 2\pi[u_k^2\delta(\epsilon + \tilde{\Delta} - \omega_k) + v_k^2\delta(\epsilon + \tilde{\Delta} + \omega_k)].$$

Here  $\xi_l = E_l - \mu_e$  and  $u_k, v_k$  and  $\omega_k$  are given by the Bogoliubov transformation. Here we consider for simplicity the term proportional to  $v_k^2$ ;  $u_k^2$  is analogous. The laser field is chosen to be a running wave, that is

$\Omega(\mathbf{x}) = \Omega e^{i\mathbf{k}_L \cdot \mathbf{x}}$ . The term  $|T_{kl}|^2$  now produces a delta-function enforcing momentum conservation. Note that this is very different from the assumption of a constant transfer matrix ( $\sum_{kl} |T_{kl}|^2 \rightarrow |T|^2 \sum_{kl}$ ) made in the standard calculation for tunneling of electrons over a superconductor – normal metal surface [25]. The final result becomes (assuming for simplicity that the temperature  $T = 0$ )

$$I = -\pi\Omega^2 \rho(\Delta) \theta(-\tilde{\Delta} - \omega_{\tilde{k}-k_L} - \Delta\mu) \frac{\omega_{\tilde{k}-k_L} - \xi_{\tilde{k}-k_L}}{\omega_{\tilde{k}-k_L} + \xi_{\tilde{k}-k_L}} \left[1 - \frac{k_L}{\tilde{k}}\right]$$

where  $\tilde{k}$  is given by the following energy conservation condition:

$$-\tilde{\Delta} + \omega_{\tilde{k}-k_L} + \xi_{\tilde{k}-k_L} = 0,$$

$\omega_k = \sqrt{\xi_k^2 + \Delta_G^2}$ , and

$$\rho(\Delta) = \frac{V}{2\pi^2} \sqrt{\frac{\Delta_G^2 - \Delta^2}{\Delta}} + 2\mu_g$$

is the density of states which appears when the summation over momenta is changed into an integration over energies.

The laser momentum  $k_L$  can be very small compared to the momentum of the atoms, especially in the case of a Raman process. By setting  $k_L = 0$  the result becomes, including now terms proportional to both  $v_k^2$  and  $u_k^2$ :

$$I = \pm \pi\Omega^2 \rho(\Delta) \theta(\Delta^2 - \Delta_G^2 + 2\Delta\mu\Delta) \frac{\Delta_G^2}{\Delta^2}, \quad (5)$$

where  $\pm$  are for  $\Delta > 0$  and  $\Delta < 0$ , respectively. The term with the  $-$  sign corresponds to  $\Delta < 0$  i.e. current from  $|g\rangle$  to  $|e\rangle$ , and the positive term to current from  $|e\rangle$  to  $|g\rangle$ . To understand the results in terms of physics, let us first consider the case of equal chemical potentials  $\Delta\mu = 0$ :

$$I = -\pi\Omega^2 \frac{\Delta_G^2}{\Delta^2} \rho(\Delta) [\theta(-\Delta - \Delta_G) - \theta(\Delta - \Delta_G)]. \quad (6)$$

In order to transfer one atom from the state  $|g\rangle$  to  $|e\rangle$  the laser has to break a Cooper pair. The minimum energy required for this is the gap energy  $\Delta_G$ , therefore the current does not flow before the laser detuning provides this energy – this is expressed by the first step function in (6). As  $|\Delta|$  increases further, the current will decrease quadratically. This is because the case  $|\Delta| = \Delta_G$  corresponds to the transfer of particles with  $p = p_F$ , whereas larger  $|\Delta|$  means larger momenta, and there are simply fewer Cooper-pairs away from the Fermi surface. This behaviour is very different from the electron tunneling where the current grows as  $\sqrt{(eV)^2 - \Delta_G^2}$  [25] (the voltage  $eV$  corresponds to the detuning  $\Delta$  in our case) because all momentum states are coupled to each other. The second step function in (6) corresponds to tunneling

into the superconductor. In this case one has to provide extra energy because a single particle tunneling into a superconductor becomes a quasi-particle excitation with the minimum energy given by the gap energy.

When the chemical potentials are not equal the situation is more complicated, but the basic features are the same: i) threshold for the onset of the current determined by the gap energy and difference in chemical potentials, and ii) further decay of the current because the density of the states that can fulfill energy and momentum conservation decreases.

## B. Harmonic confinement

In the case of harmonic confinement the spatial dependence of the current is non-trivial. We define the total current as

$$I(t) = - \int d^3x \langle \dot{N}_e(\mathbf{x}) \rangle, \quad (7)$$

where

$$\dot{N}_e(\mathbf{x}) = i[H, N_e(\mathbf{x})] = i[\Omega^*(\mathbf{x})\psi_g^\dagger(\mathbf{x})\psi_e(\mathbf{x}) - H.c.]. \quad (8)$$

No expansion in the plane waves or other basis functions is made at this point and the first order perturbation calculation leads to a result with explicitly spatially dependent correlation functions:

$$I = 2Im[X_{ret}(-\tilde{\Delta})], \quad (9)$$

where

$$X_{ret}(-\tilde{\Delta}) = i \int_{-\infty}^{\infty} dt e^{-i\tilde{\Delta}t} \theta(t) \int d^3x \times \int d^3x' \langle [A^\dagger(\mathbf{x}, 0), A(\mathbf{x}', t)] \rangle, \quad (10)$$

and

$$A(\mathbf{x}, t) = \Omega^*(\mathbf{x})\psi_g^\dagger(\mathbf{x})\psi_e(\mathbf{x}). \quad (11)$$

The retarded Green's function  $X_{ret}(-\tilde{\Delta})$  is calculated using Matsubara techniques. For performing the Matsubara summations, the spatially dependent Green's functions for the normal and the superfluid state are expanded using the trap wave functions  $\phi_n(\mathbf{x})$ , and the Bogoliubov-de Gennes (BdG) eigenfunctions  $u_n(\mathbf{x})$  and  $v_n(\mathbf{x})$ , respectively. This leads to the result

$$X_{ret}(-\tilde{\Delta}) = \int_{-\infty}^{\infty} \frac{d\epsilon}{2\pi} \int d^3x \int d^3x' \Omega^*(\mathbf{x}) \Omega(\mathbf{x}') [\tilde{A}_e(\mathbf{x}, \mathbf{x}', \epsilon) G_{adv}^g(\mathbf{x}', \mathbf{x}, \epsilon + \tilde{\Delta}) + G_{ret}^e(\mathbf{x}, \mathbf{x}', \epsilon - \tilde{\Delta}) \tilde{A}_g(\mathbf{x}', \mathbf{x}, \epsilon)], \quad (12)$$

where  $\tilde{A}_{e/g}$  are defined

$$\tilde{A}_{e/g}(\mathbf{x}, \mathbf{x}', \epsilon) = i(G_{ret}^{e/g}(\mathbf{x}, \mathbf{x}', \epsilon) - G_{adv}^{e/g}(\mathbf{x}, \mathbf{x}', \epsilon)),$$

and

$$G_{adv}^g(\mathbf{x}', \mathbf{x}, \epsilon) = \sum_n \frac{u_n(\mathbf{x}') u_n^*(\mathbf{x})}{\epsilon - \omega_n - i\delta} + \frac{v_n^*(\mathbf{x}') v_n(\mathbf{x})}{\epsilon + \omega_n - i\delta} \quad (13)$$

$$G_{ret}^e(\mathbf{x}, \mathbf{x}', \epsilon) = \sum_n \frac{\phi_n(\mathbf{x}) \phi_n^*(\mathbf{x}')}{\epsilon - \xi_n + i\delta}. \quad (14)$$

As mentioned,  $u_n(\mathbf{x})$ ,  $v_n(\mathbf{x})$  and  $\omega_n$  are given by the BdG equations [28]. In taking the imaginary part of the expression (12) we first collect together all spatially dependent terms, which gives real factors of the form  $|\int d^3x \Omega(\mathbf{x}) u_n(\mathbf{x}) \phi_m(\mathbf{x})|^2$  (we also use the fact that the trap wave functions  $\phi_m(\mathbf{x})$  are real). Imaginary parts of the remaining terms give spectral functions in the usual way. The derivation leads to

$$I = -2\pi \sum_{n,m} \left| \int d^3x \Omega(\mathbf{x}) u_n(\mathbf{x}) \phi_m(\mathbf{x}) \right|^2 [n_F(\omega_n) - n_F(\xi_m)] \delta(\xi_m + \tilde{\Delta} - \omega_n) + \left| \int d^3x \Omega(\mathbf{x}) v_n^*(\mathbf{x}) \phi_m(\mathbf{x}) \right|^2 [n_F(-\omega_n) - n_F(\xi_m)] \delta(\xi_m + \tilde{\Delta} + \omega_n). \quad (15)$$

Note that this form does not lead to a simple step-function type behaviour like in the homogeneous case. Due to the non-orthogonality of the trap and the BdG wavefunctions transitions between many quantum numbers are allowed and the total current is the sum of all these.

In the following sections we use the result (15) to investigate the feasibility of the method as a probe in different physical situations. The eigenfunctions and values  $v_n(\mathbf{x})$  and  $\omega_n$  are calculated numerically from the BdG equations using the pseudo-potential method presented in [29]. We assume for simplicity that the trap has spherical symmetry. The quantum numbers  $n, m$  in Eq.(15) then become  $\eta, l, m$  with  $l, m$  being the usual angular momentum quantum numbers. The quasi particle (QP) energies will only depend on  $\eta, l$ . The method of solving the BdG equations is described in detail in [29].

Note that the above derivation assumes that the BdG equations are solved exactly. One can, however, also use the local density approximation [30] where the chemical potential of the superconducting state is assumed to have a parametric dependence on position. In this case one should repeat the above derivation by assuming that the superfluid state Hamiltonian  $H_{gg'}$  is parametrically depended on  $\mathbf{x}$ :  $H_{gg'}^{\mathbf{x}}$ . This leads to a result identical to (15) except that now  $u_n, v_n$  are actually plane waves but they as well as  $\omega_n$  have a parametric dependence on  $\mathbf{x}$  via  $\mu(\mathbf{x})$ . We may denote the current for a chosen  $\mathbf{x}$  as  $I^{\mathbf{x}}$ . The total current is then the average of  $I^{\mathbf{x}}$  for all  $\mathbf{x}$ .

#### IV. THE EFFECT OF CHEMICAL POTENTIAL, LASER PROFILE AND TRAPPING

The behaviour of the current is strongly influenced by the choice of the physical parameters. This allows a convenient way to optimize the probing scheme as well as to investigate interesting physics such as the influence of the harmonic confinement — this is our twofold aim in the following.

Although for instance the laser profile can be chosen by will, there are a few basic restrictions in choosing the chemical potentials and the interaction strengths between the atoms in different internal states. In order for a gas of Fermionic atoms in two internal states to form Cooper pairs, the interatomic interaction should be large enough and the chemical potentials corresponding to the two states should be very close to each other [12]. This is the condition we assume for  $|g\rangle$  and  $|g'\rangle$ . The state  $|e\rangle$  is always assumed to have either negligible interaction with the states  $|g\rangle$  and  $|g'\rangle$ , or considerably lower chemical potential (smaller number of particles). It turns out that not only the pairing effects the light absorption but also normal interactions described by the Hartree-field are crucial. This is illuminated by a comparison of these two cases of  $|e\rangle$  having negligible scattering length or small chemical potential.

In real experiments, the gas is trapped in a harmonic potential. We have derived results also for the homogeneous case, these can be used in the case of very large traps and they also give a simple intuitive picture of the basic physics in this system. We will show that indeed the trapping has considerable effect on the results. On the other hand, an effectively homogeneous situation can be achieved by choosing the laser to probe only the center of the trap. As will be shown, this avoids certain problems arising from the non-homogeneous potential and can give a very clear signature of the superconducting state.

#### V. CONSTANT BEAM PROFILE

In this section we present exact numerical results in the limit when the laser beam intensity can be well approximated by a constant. That is, we take  $\Omega(\mathbf{x}) = \Omega$  in Eq.(15). As the typical effective wavelength for the laser is much larger than the extend of the trap for the relevant energies, such an approximation should be good as long as the laser amplitude is constant over the whole extend of the cloud. We present results for two situations: the case when there are no atoms initially in the state  $|e\rangle$  and the case when the chemical potentials for  $|e\rangle$  and  $|g\rangle$  are the same.

#### A. No $|e\rangle$ atoms initially

In the case considered in this subsection, we assume to have initially only a gas of interacting  $|g\rangle$  and  $|g'\rangle$  atoms. The laser beam then induces transitions to the hyperfine level  $|e\rangle$ . To obtain clear results, we will assume that the  $|e\rangle$  atoms see the same Hartree field as the  $|g\rangle$  atoms. This means that  $g_{eg} + g_{eg'} = g_{gg'}$  since the  $|e\rangle$  atoms see the Hartree field from both the  $|g\rangle$  and  $|g'\rangle$  atoms. Here,  $g_{gg'} = 4\pi a_{gg'}/m$  denotes the interaction strength between the two hyperfine states  $|g\rangle$  and  $|g'\rangle$  and likewise for  $g_{eg}$  and  $g_{eg'}$ . The parameter  $a_{gg'}$  is the usual  $s$ -wave scattering length for scattering between  $|g\rangle$  and  $|g'\rangle$  atoms. Experimentally, this situation could possibly be achieved by manipulating an external magnetic field thereby tuning the effective low energy interaction between the relevant hyperfine states to an appropriate value. In Fig. 2, we show a typical example of the current  $I(\Delta) = -\langle \dot{N}_e \rangle$ . We have used parameters such that  $g_{gg'} = -l_{ho}^3 \omega$ ,  $\mu_g = 31.5\omega$  and the temperature  $T = 0$  with  $\mu_g$  denoting the chemical potential for the  $|g\rangle$  and  $|g'\rangle$  atoms. Here  $l_{ho} = (m\omega)^{-1/2}$  is the harmonic oscillator length. For  ${}^6\text{Li}$  atoms with  $a_{gg'} = -1140\text{\AA}$  [31], this corresponds to approx.  $1.6 \times 10^4$  atoms trapped in the states  $|g\rangle$  and  $|g'\rangle$  with a trapping frequency of 820Hz yielding a critical temperature  $T_c \sim 110nK$  for the BCS transition. We have added an imaginary part  $\Gamma = 0.1\hbar\omega$  to the quasiparticle energies such that the  $\pi\delta(x)$ -functions in Eq.(15) become Lorentzians  $\Gamma/2(x^2 + \Gamma^2/4)$ .

*Normal-normal current* The dashed curve in Fig. 2 depicts the current when the  $|g\rangle$  and  $|g'\rangle$  atoms are in the normal phase. Since the  $|e\rangle$  atoms see the same Hartree-field as the  $|g\rangle$  atoms, the spatial part of the QP wavefunctions is the same for the two hyperfine states. Thus, the overlap integrals in Eq.(15) simply become  $\delta_{nm}$ -functions and since the quasiparticle spectrum is the same for the two hyperfine states, we obtain from Eq.(15):

$$I(\Delta) = -2N_g \frac{\Gamma/2}{\Delta^2 + \Gamma^2/4}. \quad (16)$$

where  $N_g$  is the number of  $|g\rangle$  atoms trapped.

*Superconductor-normal current* The solid curve Fig. 2 depicts the current when  $|g\rangle$  and  $|g'\rangle$  are in the superfluid phase. We see that the maximum of the current is displaced from  $\Delta = 0$  and that the shape of the current profile is asymmetric. Both effects are quite straightforward to understand. The asymmetry reflects the fact that the current now is given by a sum of Lorentzians centered at different frequencies since the QP spectra for  $|g\rangle$  and  $|e\rangle$  are different and the overlap integral in Eq.(15) does not give a simple selection rule. The shift in the center of the peak to negative  $\Delta$  is due to the fact that in order to induce a transition from a low lying QP-state in the superfluid one needs to break a Cooper pair. This requires an additional energy given by the pairing energy

of the QP-state. As a fraction  $\sim T_c/T_F$  of the particles participates in the pairing and they on average have the pairing energy  $T_c$ , one can estimate the order of magnitude of the shift in the center of the peak away from its normal phase value  $\Delta = 0$  to be  $\mathcal{O}(T_c^2/T_F)$ . Here,  $T_c$  is the critical temperature for the BCS transition and  $k_B T_F = \mu_g$  is the Fermi temperature for the  $|g\rangle$  atoms. For the present parameters, we have  $k_B T_c \approx 2.8\omega$  giving  $T_c^2/T_F \sim 0.25$  in qualitative agreement with the results depicted in Fig. (2). We have performed numerical calculations for several values  $g_{gg'}$  and  $\mu_g$ , and we find the general behavior as described in the present example. In all the tested cases, the current peak for the superfluid phase is shifted away to negative values of  $\Delta$  and the shape of the peak is asymmetric as opposed to the simple Lorentzian shape for the normal phase. The shift of the peak is of the order  $\mathcal{O}(T_c^2/T_F)$ .

In order to enhance the effect of the pairing on  $I(\Delta)$  even further, one could initially also trap some  $|e\rangle$  atoms. As long as  $\mu_g - \mu_e \gg \Delta_G$ , the  $|e\rangle$  atoms will not Cooper pair with the  $|g\rangle$  or  $|g'\rangle$  atoms even though  $g_{eg}$  or  $g_{eg'} < 0$  [12]. By having the lower QP states for the  $|e\rangle$  atoms filled, there will only be transitions between the QP states around the Fermi energy. Since these states are influenced the strongest by the pairing, the effect of the superfluidity on  $I(\Delta)$  will be even stronger than for the parameters relevant for Fig. 2. This is illustrated by Fig. 3, where we plot  $I(\Delta)$  for the same parameters as above apart from that now  $\mu_e = 21.5\hbar\omega$ . We see that both the asymmetry and the shift in the peak in the superfluid phase as compared to the normal phase, is more pronounced than in Fig. (2). This is simply because the transitions deep below the Fermi level which are essentially inert to the effects of superfluidity, are blocked by filling up the levels for the  $|e\rangle$  atoms up to the energy  $E = 21.5\hbar\omega$ . However, it might be somewhat more difficult to achieve this situation experimentally, as it requires the initial trapping of 3 (instead of 2) hyperfine states with a rather good control of the populations in each state.

One should note that it is important that the Hartree field seen by the  $|g\rangle$  and  $|e\rangle$  atoms is approximately the same. Otherwise, the wavefunctions and the spectra for the  $|g\rangle$  and  $|e\rangle$  atoms will be different even when the  $|g\rangle$  and  $|g'\rangle$  atoms are in the normal phase. The overlap integrals will then not give simple selection rules and there will be a contribution from many Lorentzians centered in general away from  $\Delta = 0$ . Consequently,  $I(\Delta)$  will not be given by the simple formula in Eq. (16). This is illustrated in Fig. 4, where we plot the current  $I(\Delta)$  for the same parameters as given above (with no  $|e\rangle$  atoms initially), apart from we now have  $g_{eg} + g_{eg'} = 0.9 \times g_{gg'}$ . As expected, the current profile is shifted away from  $\Delta = 0$  and is asymmetric, even when the  $|g\rangle$  and  $|g'\rangle$  atoms are in the normal phase. The shift to negative frequencies is easy to understand: The attractive mean (Hartree)

field seen by the  $|e\rangle$  atoms is smaller than the attractive field seen by the  $|g\rangle$  atoms since  $g_{eg} + g_{eg'} = 0.9 \times g_{gg'}$ . Therefore, the trap states for the  $|e\rangle$  atoms in general have a slightly higher energy than for the  $|g\rangle$  atoms, and the normal phase current is shifted to negative  $\Delta$ . Figure 4 demonstrates that the pairing field still causes a general shift of  $I(\Delta)$  to negative frequencies and introduces further asymmetry since the pairing energy still needs to be broken to generate a current from the superfluid phase. This effect is readily visible since the Hartree fields seen by the  $|g\rangle$  and  $|e\rangle$  atoms are approximately the same for the parameters chosen. However, if the difference in the Hartree fields becomes too large, the spread in the signal is determined by this difference and any additional effects coming from the pairing field are correspondingly obscured. In general, to be able to detect the presence of superfluidity using the scheme described in this section, one should have  $\Delta W \ll \Delta_G$  where  $\Delta W = |g_{gg'} - g_{eg} - g_{eg'}|\rho$  denotes the difference in the Hartree fields with  $\rho$  being the average density of the  $|g\rangle$  atoms, and  $\Delta_G$  is the average gap.

We conclude that if  $g_{eg} + g_{eg'} = g_{gg'}$  to a very good approximation so that the difference in the Hartree fields seen by the  $|g\rangle$  and the  $|e\rangle$  is negligible, the effect of superfluidity on the current  $I(\Delta)$  should be straightforward to observe. The current in the normal phase is a simple Lorentzian centered around  $\Delta = 0$ , whereas in the superfluid phase it is asymmetric and shifted away from  $\Delta = 0$ . Furthermore, the shift in the center of the peak provides an estimate of  $T_c$  if  $T_F$  is known. Both the asymmetry and the shift away from  $\Delta = 0$  should be easily observable indications of the presence of superfluidity. The effect is further enhanced if one initially traps  $|e\rangle$  atoms keeping  $\mu_g - \mu_e \gg \Delta_G$ . In general, the scheme described in this section requires that the difference in the Hartree fields seen by the  $|g\rangle$  and the  $|e\rangle$  is smaller than the average pairing field in order to obtain a visible effect of the superfluidity on the current.

## B. Equal chemical potentials

We now consider the case of  $\mu_e \simeq \mu_g$ , where there is initially many atoms trapped in the state  $|e\rangle$ . Hence, to avoid the otherwise interesting possibility of the  $|e\rangle$  atoms participating in the pairing, we assume that  $g_{eg} = g_{eg'} = 0$ . In Fig. 5, we plot the current  $I(\Delta)$  for  $g_{gg'} = -l_{ho}^3\omega$ ,  $\mu_e = \mu_g = 31.5\omega$ ,  $T=0$ , and  $g_{eg} = g_{eg'} = 0$ . We have taken  $\Gamma = 0.1\omega$ . As can be seen, there are several peaks in  $I(\Delta)$  both when  $|g\rangle$  and  $|g'\rangle$  are in the normal phase and when they are in the superfluid phase. In both cases, the peaks simply correspond to individual QP energy bands overlapping.

To see this, we plot in Fig. 6 the corresponding lowest QP energies for the  $|e\rangle$ ,  $|g\rangle$ , and  $|g'\rangle$  atoms in both phases as a function of their angular momentum  $l$ . As we are

in the Bogoliubov picture, all QP energies are positive and measured relative to the chemical potential. In the normal phase, negative QP energies  $\xi_n = \epsilon_n - \mu < 0$  are represented as positive QP energies  $E_n = |\xi_n|$  with hole character. In Fig. (6), we label a hole-state by  $\circ$  whereas a particle state is indicated by a  $\times$ . In the superfluid phase, the QP's are in general a superposition of a hole and a particle which we label by  $+$ .

We see that when the Hartree field is attractive, a normal phase energy band with a downward curvature in Fig. 6 is a hole band whereas a normal phase energy band with an upward curvature is a particle band. The reason is that particle states with lower angular momentum  $l$  has a lower energy for an attractive interaction ( $g < 0$ ) than states with a higher  $l$  since the wavefunction overlap with the Hartree field decreases with increasing  $l$  [4].

The QP bands for the  $|e\rangle$  atoms are flat as they are the simple unperturbed harmonic oscillator states with energies  $E_n = |(n + 3/2)\omega - \mu_e|$ . The lowest  $E = 0$  band corresponds to the harmonic oscillator states at the chemical potential ( $n = 30$ ) with angular momentum  $l = 0, 2, \dots, 30$ . The interpretation of the spectra is described in detail in [4,20]. There is a one to one correspondence between the peaks in Fig. 5 and the QP bands depicted in Fig. 6. For instance, the broad peak centered around  $\Delta = \omega$  when the  $|g\rangle$  and  $|g'\rangle$  atoms are in the normal phase corresponds to transitions from the half-filled QP band at  $E = 0$  for the  $|e\rangle$  atoms into the empty (particle) band with  $0.5 \lesssim E/\omega \lesssim 1.8$  for  $l = 0, 2, \dots, 30$  for the  $|g\rangle$  atoms in the normal phase.

We note that the peaks for the superfluid phase are sharper than the peaks for the normal phase. This is because the lowest QP bands for the  $|g\rangle$  atoms are almost degenerate as a function of  $l$  in the superfluid phase as can be seen from Fig. 6. These states are strongly influenced by the pairing field, which “pushes” them away from the center of the trap. They are concentrated in the region between where the pairing field and the trapping potential are significant [18,20], and they thus do not feel the Hartree field. Therefore, their dependence on the quantum number  $l$  is much weaker than in the normal phase.

We have performed calculations for a number of different parameters and we have observed the general behavior of  $I(\Delta)$  as described above. We conclude that when we have  $\mu_e \simeq \mu_g$  and  $g_{eg} = g_{eg'} = 0$ , the presence of superfluidity is somewhat harder to detect as compared to the situation described in sec. V A. This is because the Hartree field tends to obscure any additional effect coming for the pairing. The current  $I(\Delta)$  has in general many peaks corresponding to the energetic overlap between individual QP bands for the  $|e\rangle$  and the  $|g\rangle$  atoms both for the normal and the superfluid phases. The effect of the superfluidity is to make the peaks sharper than in the normal phase since the pairing field tends restore the degeneracy in the QP energies with respect to the angu-

lar momentum. One could therefore possibly detect the onset of superfluidity as a sharpening of the peaks.

## VI. PROBING THE CENTER OF THE TRAP – EFFECTIVELY HOMOGENEOUS SYSTEM

We now assume that the laser intensity  $\Omega(\mathbf{x})$  is large in the center of the cloud and that it decreases quickly as a function of the distance from the center of the trap. This situation can be experimentally achieved by using a Raman transition scheme with two perpendicular laser beams crossing each other at the center of the cloud. The profile of each laser beam should be narrow on the length scale of the trapped cloud. Since the laser beams then effectively probe only atoms in the center of the cloud where the Hartree and pairing fields are approximately constant, we would expect the observed signal to be well described by the results for a homogeneous system as given by Eq.(5). From section III A, we conclude that, for a homogeneous system, the optimal way of detecting the presence of the pairing field is to have  $\mu_g \simeq \mu_e$  (see Eq.(6)). In this limit, all low lying transitions far away from the Fermi energy and thus very little affected by the pairing, are Fermi blocked. The transitions contributing to  $I(\Delta)$  are all close to the Fermi level and hence strongly influenced by the presence of the pairing field. We will therefore concentrate on the case where the effective chemical potential in the center of the trap is the same for  $|g\rangle$  and  $|e\rangle$ . As we will see, this case opens up the interesting possibility of directly measuring the size of the gap in the center of the cloud.

We use the same set of parameters as in sec. V B for the  $|g\rangle$  and  $|g'\rangle$  atoms. But now we assume that the intensity profile for the beam can be well approximated by a sphere of constant intensity for  $r \leq r_0$  and zero intensity for  $r > r_0$  with  $r$  denoting the distance to the center of the trap. That is, we take  $\Omega(\mathbf{r}) = \Omega\Theta(r_0 - r)$  in Eq.(15) with  $r_0 = 2l_{ho}$ . From Fig. 7, we see that  $\Delta_G(r) \simeq 6\omega$  and  $W(r) \simeq 15\omega$  for  $r \leq 2l_{ho}$ . Thus, the effective local potential for the  $|g\rangle$  atoms is  $\mu_g \sim 46.5\omega$ . We therefore take  $\mu_e = 46.5\omega$  and  $g_{eg} = g_{eg'} = 0$  in order to have the same effective local chemical potential for  $|g\rangle$  and  $|e\rangle$  in the center of the trap. The result is shown in Fig. 8. Since the system is approximately homogeneous for  $r \leq 2l_{ho}$ , one could expect the current profile to be well described by Eq.(6), with  $\mu_e = \mu_g = 46.5\omega$  and  $\Delta_G = 6\omega$ . We therefore also plot the result predicted by Eq.(6). Here we take  $\mu_e = \mu_g = 46.5\omega$  and  $\Delta_G = 6\omega$  and we have normalized  $I(\Delta)$  to a volume of  $V = 4\pi r_0^3/3$ . We have taken a rather large value of  $\Gamma = 1\omega$  such that the discrete nature of the trap spectrum is washed out. Note that a finite imaginary part  $\Gamma$  to the QP energies corresponds to convoluting Eq.(6) with a Lorentzian of width  $\Gamma$ .

As can be seen, there is a good agreement between the exact numerical result and the prediction based on Eq.(6). Especially, the current is zero for  $-6\omega \lesssim \Delta \lesssim 6\omega$  as predicted by Eq.(6), since one either needs to break a Cooper pair with pairing energy  $\sim \Delta_G(r=0)$  to produce a current into  $|e\rangle$  ( $\Rightarrow \Delta \lesssim -6\omega$ ) or one has to create a QP with energy minimum  $\sim \Delta_G(r=0)$  ( $\Rightarrow \Delta \gtrsim 6\omega$ ) to generate a current into  $|g\rangle$ . The peaks in the numerical result reflect, of course, the discreteness of the trap levels. These peaks are quite large, as there is only  $\approx 500$  particles trapped in the region  $r \leq 2l_{ho}$  for the parameters given above. Clearly, these peaks cannot be reproduced by the homogeneous treatment given by Eq.(6) which however reproduces the general shape of the current profile well. If we had chosen a larger system the individual peaks would be more numerous and smaller on the scale of the gap  $\Delta_G(r=0)$  and the agreement between the homogeneous approximation and the exact result would probably be even better.

We conclude that by concentrating the beam intensity to the center of the cloud where the gas can be to a good approximation regarded as homogeneous, the current profile  $I(\Delta)$  is well described by the results presented in section III A. An important result is that by adjusting the parameters such that the local chemical potentials are the same [ $\mu_g - W_g(r=0) \simeq \mu_e - W_e(r=0)$ ], one should be able to measure directly the size of the gap in the center of the cloud. It is simply given by the threshold detuning energy below which the observed current should be zero: for  $|\Delta| \lesssim \Delta_G$  the current  $I(\Delta) \simeq 0$ .

## VII. CONCLUSIONS

The observation of the predicted BCS-state in gases of trapped atomic Fermions poses a double challenge: the order parameter is small thus a sensitive probe has to be found, furthermore, the trapping potential leads to appearance of in-gap low-energy excitations which may make it difficult to resolve the gap energy. In this paper we have presented a method which is based on the transfer of atomic population over a superconductor - normal state interface. This interface is effectively created by using a laser to couple internal states with large and small scattering lengths. The population transfer requires to break a Cooper pair and the extra energy for this is provided by the laser detuning. The change in the atomic population as a function of the laser detuning thus gives information about the gap energy. We have derived the current of population both in the case of a trapped gas and a homogeneous system, and investigated the feasibility of the method in different physical regimes.

We found that, in the case of a constant laser profile, the clearest signatures of the BCS-state are observed when it is assumed that there are initially no atoms in

the normal state. Furthermore, the scattering length between the normal state atoms and the Cooper paired ones is assumed to be about the half of the scattering length between the two Cooper paired ones – this causes all the atoms to see the same Hartree field. In this physical situation the effect of the BCS-state is particularly simple and clear: the maximum in the current of population as a function of the detuning is shifted and the peak becomes asymmetric. Although this would probably be the optimal choice, other initial conditions and probe parameters lead to clear signatures of the BCS-state as well.

To avoid the problems arising from the non-homogeneous trapping potential we propose to probe only the middle of the trap. The order parameter is effectively homogeneous in the middle and the wave-functions of the in-gap excitations are located away from the center. In practice this kind of probing can be done by using two orthogonal Raman beams which intersect only in the middle of the trap. We have shown that indeed this leads to a result very similar to the one in the homogeneous: the maximum of the current is shifted exactly by the amount of the gap energy. This allows a direct measurement of the gap energy.

*Acknowledgements* PT and MR acknowledge the support by the Academy of Finland (Projects No. 48845, No. 47140 and No. 44897 Finnish Centre of Excellence Programme 2000-2005). Work at the University of Innsbruck is supported by the Austrian Science Foundation and EU TMR networks. P.T. started this work as a Marie Curie Fellow of the EU in the University of Innsbruck.

- 
- [1] B. DeMarco and D.S. Jin, Science **285**, 1703 (1999).
  - [2] M.-O. Mewes, G. Ferrari, F. Schreck, A. Sinatra, and C. Salomon, Phys. Rev. A **61**, 011403(R) (2000).
  - [3] K.M. O'hara, M.E. Gehm, S.R. Granade, S. Bali, and J.E. Thomas, Phys. Rev. Lett. **85**, 2092 (2000).
  - [4] G. M. Bruun and K. Burnett, Phys. Rev. A **58**, 2427 (1998).
  - [5] Tin-Lun Ho, cond-mat/0005508.
  - [6] G. M. Bruun and C. W. Clark, Phys. Rev. Lett. **83**, 5415 (1999).
  - [7] L. Vichi and S. Stringari, Phys. Rev. A **60**, 4734 (1999).
  - [8] A. Csordás and R. Graham, cond-mat/0007049.
  - [9] G. Ferrari, Phys. Rev. A **59**, R4125 (1999); L. Vichi, cond-mat/0006305.
  - [10] J. Ruostekoski and J. Javanainen, Phys. Rev. Lett. **82**, 4741 (1999).
  - [11] T. Busch, J. R. Anglin, J. I. Cirac and P. Zoller, Europhys. Lett. **44**, 1 (1998).
  - [12] H.T.C. Stoof, M. Houbiers, C.A. Sackett, and R.G. Hulet, Phys. Rev. Lett. **76**, 10 (1996).
  - [13] L. You and M. Marinescu, Phys. Rev. A **60**, 2324 (1999).
  - [14] For recent reviews, see E.A. Cornell, J.R. Ensher, and



- C.E. Wieman, cond-mat/9903109; W. Ketterle, D.S. Durfee, and D.M. Stamper-Kurn, cond-mat/9904034.
- [15] F. Weig and W. Zwerger, Europhys. Lett. **49**, 282 (2000).
- [16] W. Zhang, C.A. Sackett, and R.G. Hulet, Phys. Rev. A **60**, 504 (1999).
- [17] J. Ruostekoski, Phys. Rev. A **60**, R1775 (1999).
- [18] M.A. Baranov, JETP Lett. **70**, 396 (1999).
- [19] M.A. Baranov and D.S. Petrov, cond-mat/9901108.
- [20] G.M. Bruun and C.W. Clark, cond-mat/990392 (to be published in J. Phys. B, Special issue on Coherent matter waves, November 2000).
- [21] F. Zambelli and S. Stringari, cond-mat/0004325.
- [22] A. Minguzzi and M.P. Tosi, cond-mat/0005098.
- [23] K.G. Petrosyan, JETP Letters **70**, 11 (1999).
- [24] P. Törmä and P. Zoller, Phys. Rev. Lett. **85**, 487 (2000).
- [25] G.D. Mahan, *Many-Particle Physics* (Plenum Press, New York, 1990).
- [26] J.L. Bohn, Phys. Rev. A **61**, 053409 (2000).
- [27] J. Williams, R. Walser, J. Cooper, E. Cornell, and M. Holland, Phys. Rev. A **59**, R31 (1999).
- [28] P.G. de Gennes, *Superconductivity of Metals and Alloys*, (Addison-Wesley Publishing Company, 1989).
- [29] G. Bruun, Y. Castin, R. Dum, and K. Burnett, Eur. Phys. D **7**, 433 (1999).
- [30] M. Houbiers, R. Ferweda, H.T.C. Stoof, W.I. McAlexander, C.A. Sackett, and R.G. Hulet, Phys. Rev. A **56**, 4864 (1997).
- [31] E. R. I. Abraham, W. I. Alexander, J. M. Gerton, R. G. Hulet, R. Coté, A. Dalgarno, Phys. Rev. A **55**, R3299 (1997).

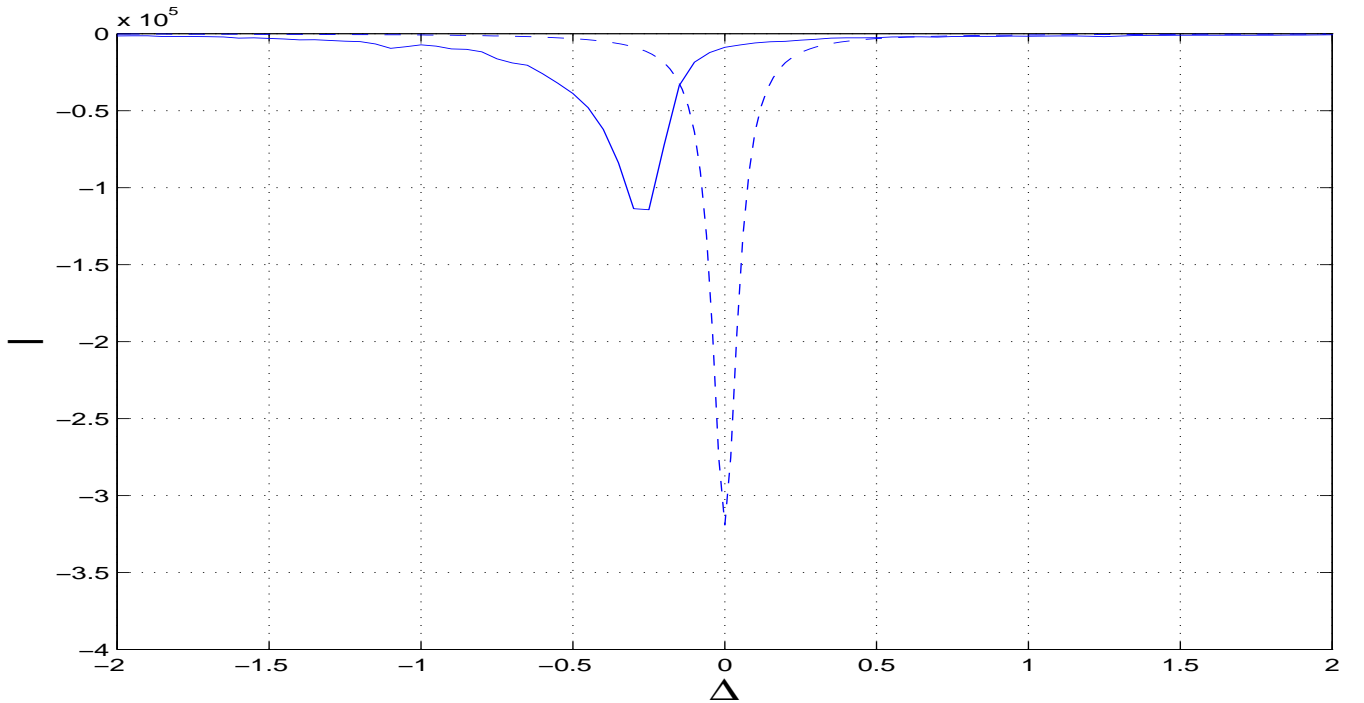


FIG. 2. The current  $I = -\langle \dot{N}_e \rangle$  as a function of the laser detuning for  $\mu_g = 31.5$ ,  $\mu_e = 0$  (in units of  $\omega$ ), and  $g_{eg} + g_{eg'} = g_{gg'}$ .

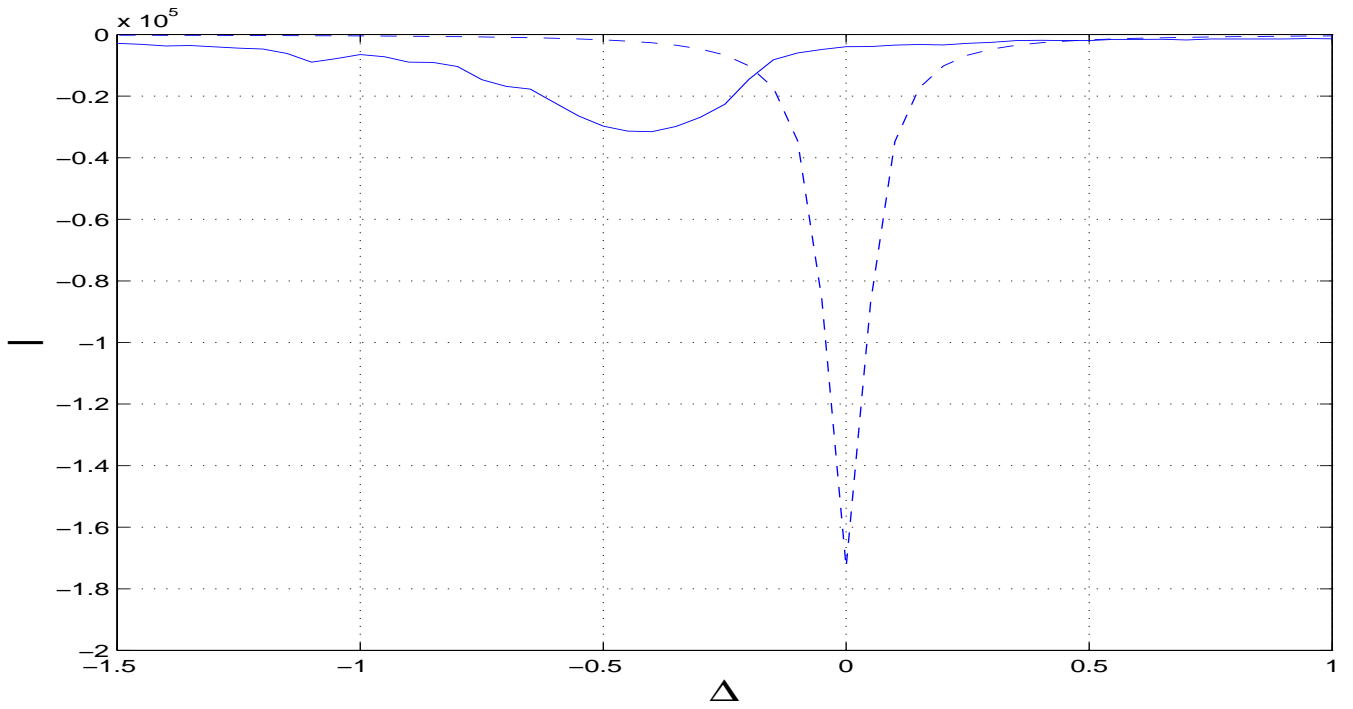


FIG. 3. The current  $I = -\langle \dot{N}_e \rangle$ . The solid/dashed lines are for the  $|g\rangle$  and  $|g'\rangle$  atoms in the superfluid/normal phase for  $\mu_g = 31.5$ ,  $\mu_e = 21.5$  (trap units), and  $g_{eg} + g_{eg'} = g_{gg'}$ .

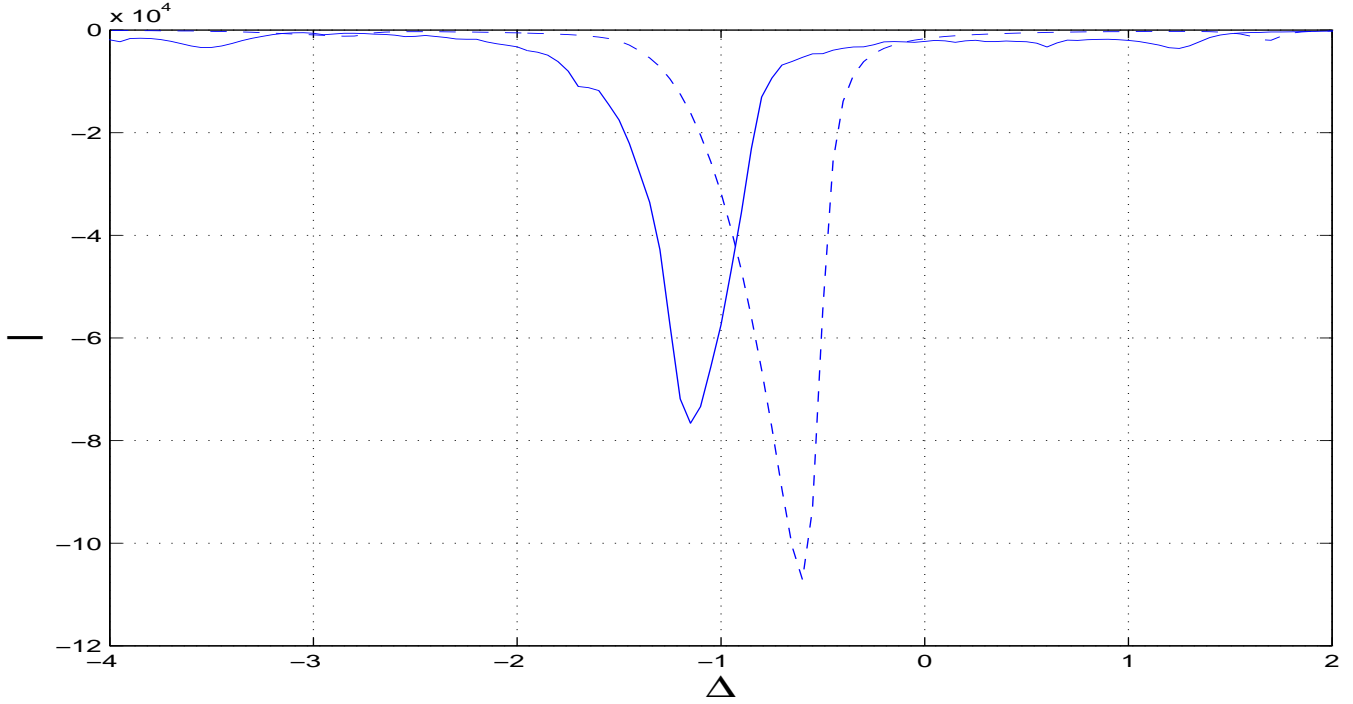


FIG. 4. The current  $I = -\langle \dot{N}_e \rangle$ . The solid/dashed lines are for the  $|g\rangle$  and  $|g'\rangle$  atoms in the superfluid/normal phase for  $\mu_g = 31.5$ ,  $\mu_e = 0$  (trap units), and  $g_{eg} + g_{eg'} = 0.9 \times g_{gg'}$ .

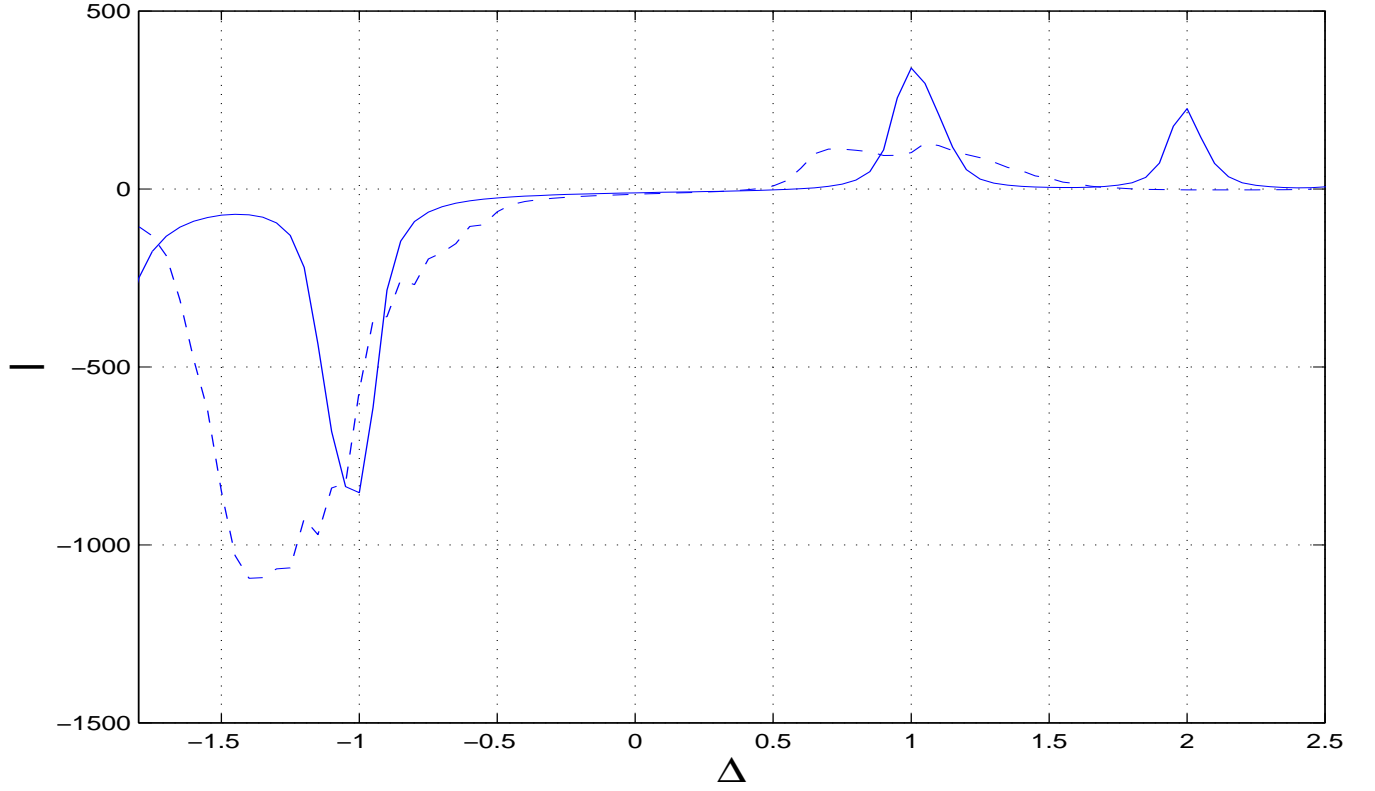


FIG. 5. The current  $I = -\langle \dot{N}_e \rangle$ . The solid/dashed lines are for the  $|g\rangle$  and  $|g'\rangle$  atoms in the superfluid/normal phase. Here  $\mu_g = \mu_e = 31.5$  (trap units),  $g_{eg} = g_{eg'} = 0$ .

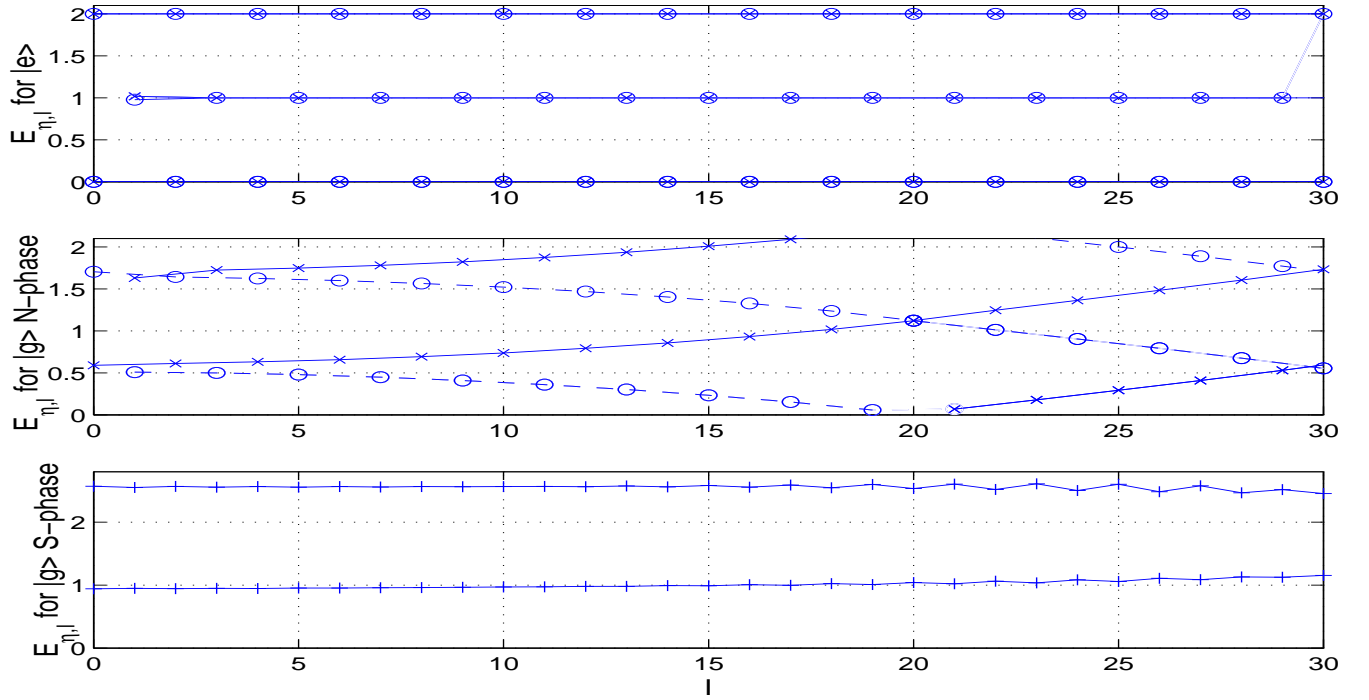


FIG. 6. The lowest QP energies  $E_{\eta,l}$  as a function of the angular momentum  $l$ , parameters are the same as in Fig. 4.

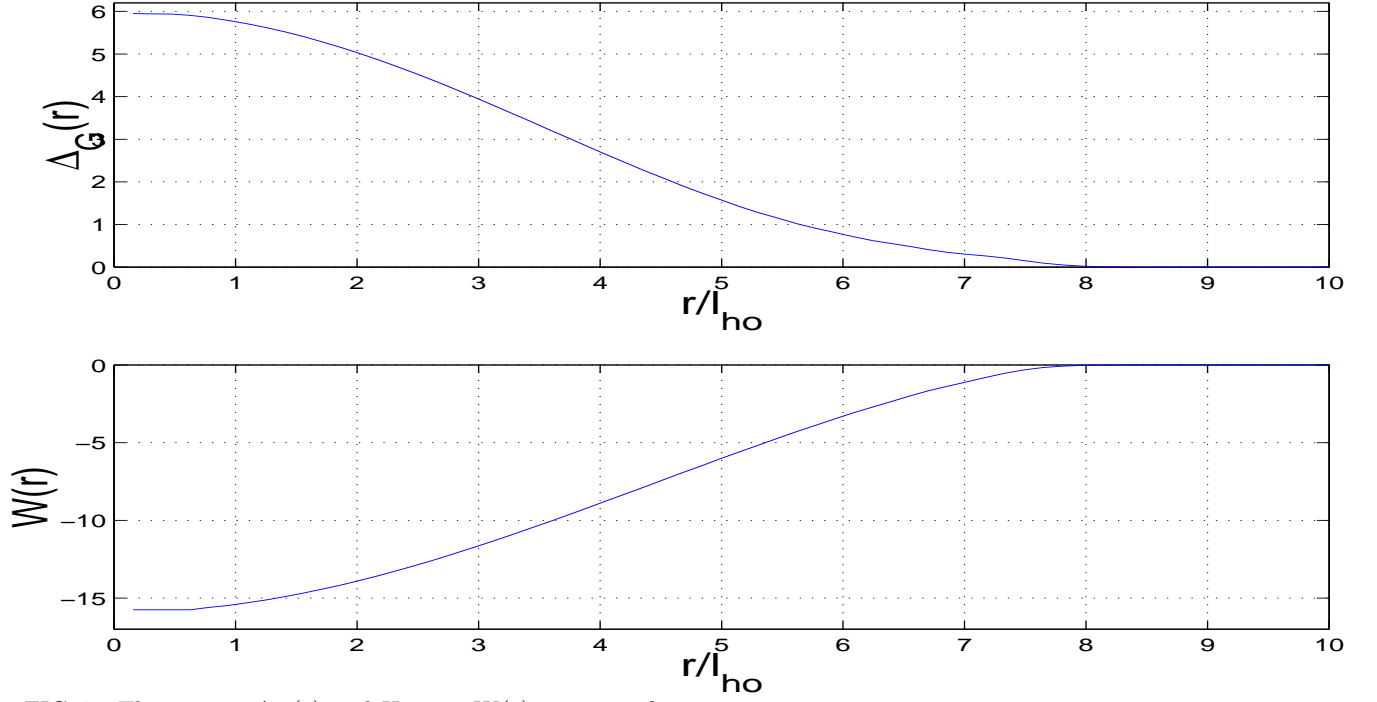


FIG. 7. The pairing  $\Delta_G(r)$  and Hartree  $W(r)$  in units of  $\omega$ , parameters are the same as in Fig. 4.

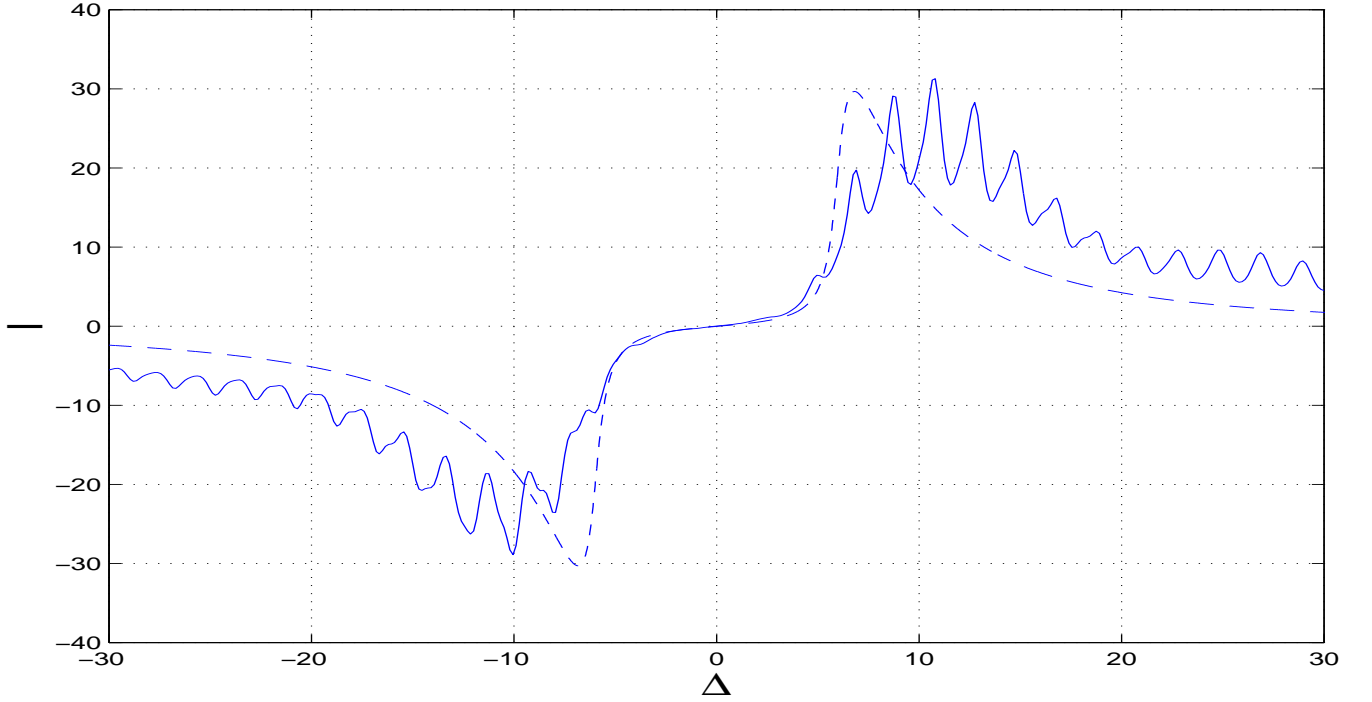


FIG. 8. The current  $I = -\langle \dot{N}_e \rangle$  for  $\mu_g = \mu_e = 46.5$  (trap units) and  $g_{eg} = g_{eg'} = 0$ . The solid line is the exact numerical result whereas the dashed line is based on Eq.(6), with  $\Delta_G = 6$ .